Adsorption and Reaction of Aldehydes on Pd Surfaces

Ratna Shekhar† and Mark A. Barteau*

Center for Catalytic Science and Technology, Department of Chemical Engineering, University of Delaware, Newark, Delaware 19716

Russell V. Plank and John M. Vohs

Department of Chemical Engineering, University of Pennsylvania, Philadelphia, Pennsylvania 19104

Received: March 27, 1997; In Final Form: July 28, 1997[⊗]

Aldehydes have been proposed as important intermediates during alcohol synthesis on supported transition metal catalysts. To develop insights into higher oxygenate syntheses, adsorption and reaction of aldehydes on transition metal surfaces and the surface structure dependence of these processes are considered here. In this work, the adsorption and reactions of acetaldehyde and propionaldehyde on Pd(110) surfaces were investigated with temperature-programmed desorption (TPD) and high-resolution electron energy loss spectroscopy techniques. The slate of desorption products observed in TPD experiments following acetaldehyde adsorption on the clean Pd(111) and Pd(110) surfaces was the same: CO, H_2, CH_4, and CH_3CHO were observed in both cases. Likewise, propionaldehyde decomposition gave rise to CO, H_2, C_2H_4, and C_2H_6 on both surfaces. However, acetaldehyde isotope-labeling experiments indicated that methyl groups were released following decarbonylation reactions of acetaldehyde on Pd(110), in contrast with earlier suggestions of methylene release on the clean Pd(111) surface. Further studies on H- and D-precovered Pd(110) surfaces elucidated the competing decomposition and hydrogenation pathways as well as the distribution of hydrocarbon species released after decarbonylation of adsorbed aldehydes on Pd(110). These results demonstrate that a variety of surface hydrocarbon ligands can be produced by aldehyde decarbonylation on palladium surfaces and imply that higher oxygenate synthesis by carbonylation of surface hydrocarbon fragments may involve an equally large variety of hydrocarbon intermediates on supported metal catalysts.

1. Introduction

It has been proposed that the formation of acyl ligands via CO insertion into hydrocarbon−surface bonds on metals and the subsequent acyl hydrogenation to produce aldehydes are critical steps in oxygenate synthesis.[1−3] The aldehydes thus formed could either hydrogenate further to produce alcohols or simply desorb as products. A number of mechanisms for higher alcohol synthesis have been proposed that identify aldehydes as important intermediates.[1−3] The selectivity for alcohol synthesis via aldehyde intermediates on the catalyst surface depends on the competition between aldehyde desorption and reaction. A complete understanding of aldehyde adsorption and reaction on transition metal surfaces is essential for developing insights into higher oxygenate synthesis from CO and H_2. Relatively few studies of higher aldehydes on model metal surfaces have previously been reported.[4−9] Aldehydes can adsorb on metal surfaces through the oxygen lone pair electrons in a η^1(O) configuration or in a η^2(C,O) configuration where both the carbonyl carbon and oxygen atoms interact with the surface metal atoms. In the first coordination type, the η^1(O) configuration, electron donation from the oxygen lone pair produces a weak surface−aldehyde bond, and as a result aldehydes adsorbed on metal surfaces in an η^1(O) configuration tend to desorb intact at low temperatures, typically ca. 200 K on Pd(111).[4] However, aldehydes in the η^2(C,O) state bind to the surface through the carbonyl π orbital, with overlap between the metal d electrons and the carbonyl π* orbital. This type of back-bonding in the η^2 configuration results in stronger metal−aldehyde bonding which ultimately leads to the competition between desorption and decomposition reactions on the surface. In fact, the preferred mode of aldehyde adsorption on Group VIII metal surfaces[4−9] is the η^2 configuration, with some η^1 species present at low temperature.

Decarbonylation of adsorbed η^2-acetaldehyde and η^2-propionaldehyde on Pd(111) was shown to proceed through stable acyl species and resulted in the production of CO, H_2, and a hydrocarbon one carbon atom shorter than the parent aldehyde.[4] The observation of a kinetic isotope effect in CH_3CHO and CD_3CDO reactions on Pd(111)[4] led to the assertion that the η^2-acetaldehyde decomposition took place via an unstable ketene species which released methylene on the surface; this observation is in excellent agreement with the suggested mechanism for the synthesis of C_2 oxygenates from syngas (CO + H_2), using supported palladium catalysts.[10,11] It is well-known that palladium is not suitable to catalyze the formation of C_2 oxygenates from syngas due to its inability to adsorb CO dissociatively. However, Ponec and co-workers[10,11] reported formation of significant yields of acetaldehyde and ethanol with Pd/V_2O_3 catalyst when CH_2Cl_2 was also added to the syngas mixture; C_2 oxygenates were not observed when CH_3Cl was added instead. These experiments by Ponec and co-workers,[10,11] which were based on the assumption that co-fed CH_2Cl_2 released CH_2 species on the surface, indicated that acetaldehyde and ethanol formation proceeded via CO addition to methylene adspecies to form ketene (CH_2═C═O) which hydrogenated to produce acetyl and then underwent further hydrogenation to produce acetaldehyde and ethanol. The mechanistic conclusions from the above studies on supported catalysts[10,11] are summarized as Scheme 1. The exact microscopic reverse of the

* Corresponding author. Fax: (302)-831-2085. E-mail: barteau@che.udel.edu.

† Present address: Novartis Pharmaceuticals Corporation, 59 Route 10, East Hanover, NJ 07936.

⊗ Abstract published in *Advance ACS Abstracts,* September 15, 1997.

S1089-5647(97)01077-8 CCC: $14.00

SCHEME 1

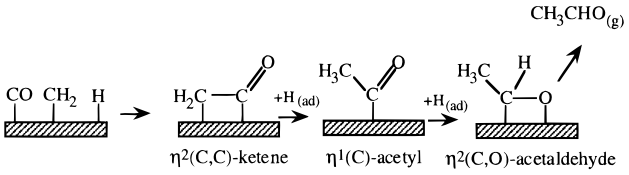

above reaction pathways (Scheme 1), under ultrahigh vacuum (UHV) conditions, was observed by Davis and Barteau[4] in their temperature-programmed desorption (TPD) and high-resolution electron energy loss spectroscopy (HREELS) studies of acetaldehyde decomposition on clean Pd(111). The mechanistic accord between UHV-based surface science investigations of acetaldehyde reactions on clean Pd(111)[4] and those of acetaldehyde synthesis on supported palladium catalysts[10,11] may in part reflect the surface structural similarity in these two examples, as the most stable surface structure in supported catalyst systems is the (111) plane.[12]

In contrast to the acetaldehyde decomposition pathways deduced on Pd(111),[4] the absence of any kinetic isotope effect during acetaldehyde decomposition on Rh(111) was reported and it was proposed that decarbonylation preceded dehydrogenation, thus releasing methyl species on the surface.[8] The competition between C−C and C−H scission in acetaldehyde adspecies on Pd(111) and Rh(111)[4,8] suggests the need for further investigation of electronic and/or geometrical influences on bond activation sequences during oxygenate decomposition on transition metal surfaces. Given the dearth of studies of higher aldehyde reactions on model transition metal surfaces, it is not surprising that there are no reported studies of possible structure sensitivity of aldehyde chemistry on Pt-group metals. The purpose of the present investigation was not only to elucidate aldehyde adsorption modes and decomposition pathways on Pd(110) but also to compare our findings with previous studies on Pd(111).[4] This work is the continuation of our efforts in exploring the issue of structure sensitivity of bond activation sequences in oxygenate reactions on Pd surfaces.[13−15] Adsorption and reaction of acetaldehyde and propionaldehyde were studied first on the clean Pd(110) surface and later, aldehyde reactions on hydrogen- and deuterium-precovered surfaces were examined to identify the hydrocarbon fragments released by decarbonylation. HREELS spectra were collected to identify the various adsorption states on the clean Pd(110) surface and also the reaction intermediates stable at different temperatures.

2. Experimental Section

Two different UHV chambers were used in this study. All TPD results were obtained in a stainless steel UHV chamber[16] equipped with a differentially pumped quadrupole mass spectrometer (UTI 100C) multiplexed with an IBM PC. The HREELS experimental apparatus and procedures employed in these studies were the same as those discussed elsewhere.[17] The reactants were dosed onto the palladium single-crystal surfaces through stainless steel needles attached via leak valves to the dosing manifold where the liquid samples under study were contained in glass tubes. Acetaldehyde (Aldrich, 99%), acetaldehyde-d_4 (MSD Isotopes, 99.6%), and propionaldehyde (Alfa, 99%) were further purified by repeated freeze−pump−thaw cycles. Mass fragmentation patterns for the parent molecules under study were regularly collected in order to verify sample purity. Research grade hydrogen and deuterium (from Matheson) were used. A sample heating rate of 3.7 ± 0.1 K/s was used in all TPD experiments. During initial TPD experiments for each probe molecule, as many as 80 *m*/*e* ratios were monitored simultaneously to identify all possible reaction products. The method of exposure and absolute surface coverage calculations have previously been discussed in detail.[13] HREELS spectra were collected in the specular mode with a beam energy of 4 eV and a resolution of 25−35 cm^{-1}; the elastic peak intensity was of the order of 100 000 counts/s. Spectra in the temperature-programmed HREELS experiments were always collected at ca. 125 K after annealing the sample for 2 min at the indicated temperature.

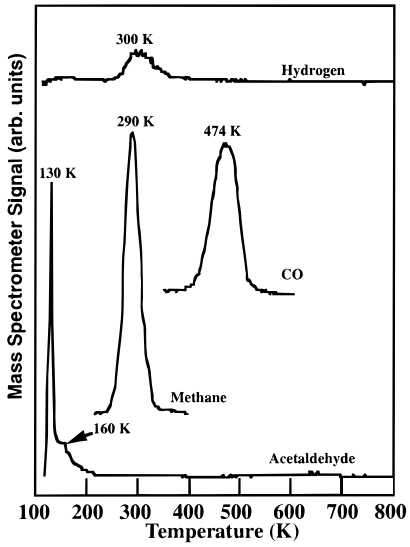

Figure 1. TPD spectra after a saturation acetaldehyde exposure (13.2 L) onto the initially clean Pd(110) surface at 120 K.

3. Results

3.1. TPD and HREELS of Acetaldehyde on Pd(110) Surfaces. Similar to results obtained on Pd(111),[4] acetaldehyde adsorbed on Pd(110) decomposed to produce methane, CO, hydrogen, and small amounts of surface carbon. Figure 1 depicts TPD spectra for these products following saturation exposure of acetaldehyde on an initially clean Pd(110) surface at 120 K. Multilayer acetaldehyde desorption took place at 130 K. For subsaturation coverages, acetaldehyde desorbed at ca. 180 K, with a small high-temperature shoulder at ca. 255 K. The acetaldehyde desorption peak from the chemisorbed state shifted to 160 K with increasing surface coverage. Different acetaldehyde desorption states with increasing exposures are indicated in Figure 2; at intermediate exposures desorption from the chemisorbed state was not well-resolved from the low-temperature multilayer state. The nature of the high-temperature shoulder at 255 K was not clear at first, and we will return to this observation after describing the acetaldehyde isotope-labeling studies. Higher temperature acetaldehyde desorption assignable to the η^2 state was not detected, unlike that observed from the Pd(111) surface.[4] In a previous study of acetaldehyde adsorption on Pd(111) at 170 K,[4] unreacted acetaldehyde desorbed in two peaks, one at 220 K (η^1-acetaldehyde) and the second, accounting for nearly one-third of the adsorbed layer, at 325 K (assigned to acetaldehyde adsorbed in the η^2 state). However, the contrasting behavior of acetaldehyde desorption states on Pd(110) vs Pd(111) surfaces is in agreement with differences observed in the behavior of higher aldehydes (acrolein[13] and propionaldehyde) on the two surfaces, as discussed below. The remaining adsorbed acetaldehyde decomposed to produce CH_4 (290 K), H_2 (300 K), CO (474 K), and a small amount of surface carbon (surface carbon was detected and quantified as the CO_2 and CO produced in subsequent oxygen adsorption/temperature-programmed de-

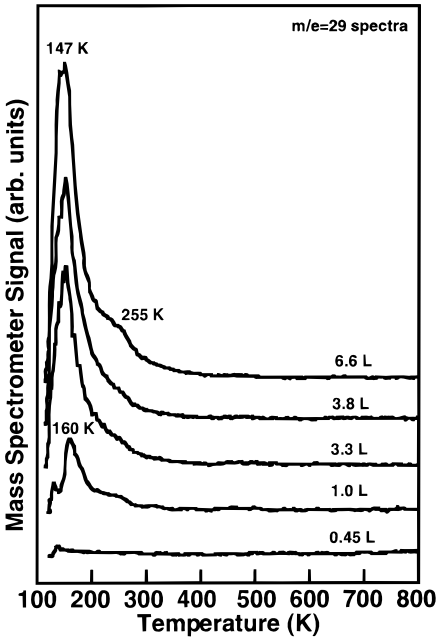

Figure 2. Series of $m/e = 29$ spectra in TPD after the indicated exposure of acetaldehyde onto the initially clean Pd(110) surface at 120 K.

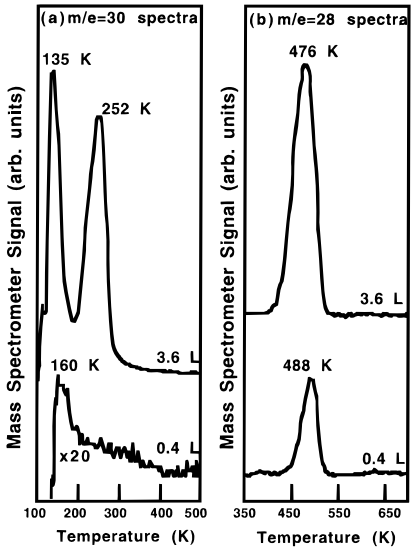

Figure 3. (a) $m/e = 30$ spectra monitoring acetaldehyde-d_4 desorption; (b) $m/e = 28$ spectra monitoring the amount of CO produced following decarbonylation after the indicated exposures of acetaldehyde-d_4 on Pd(110) at 120 K.

sorption cycles, as previously described[13]). The evolution of H_2 and CO during acetaldehyde TPD was, in each case, desorption-limited.[18,19] The total amount of acetaldehyde adsorbed on Pd(110) at 120 K was one-third monolayer (ML) and nearly 20% of the acetaldehyde adlayer desorbed from the chemisorbed state on Pd(110). Yields corresponding to the acetaldehyde TPD spectra shown in Figure 1 were 0.26 ML of CO, 0.24 ML of methane, 0.04 ML of hydrogen, and roughly 0.02 ML of surface carbon. The CH_4/CO yield ratio in acetaldehyde TPD was 0.95 and hardly any hydrogen desorption was observed above 400 K. In the case of Pd(111),[4] 72% of the adsorbed acetaldehyde decarbonylated, producing methane and CO with a ratio of 0.8. The remainder of the methyl groups originally present in acetaldehyde dehydrogenated completely to hydrogen and surface carbon at ca. 410 K on Pd(111). Methane desorption took place at 290 K on the Pd(110) surface, as observed for ethanol decomposition which proceeds via an acetaldehyde intermediate on this surface.[14] No evidence for any C_2-hydrocarbon desorption or formation during the acetaldehyde reaction was observed in either spectrum. Saturation acetaldehyde coverages on both Pd(110) and Pd(111) surfaces were approximately one-third of the respective monolayers; however, the fraction decarbonylated on Pd(110) was higher.

TPD after a acetaldehyde-d_4 dose onto the initially clean Pd(110) surface at 120 K resulted in D_2, CO, methane isotopomers, and little surface carbon. The desorption peak temperatures for volatile products following acetaldehyde-d_4 TPD were the same as those following nondeuterated acetaldehyde TPD on Pd(110). TPD results for two limiting coverages (high and low coverage) are shown in Figure 3. TPD following a 3.6 L acetaldehyde-d_4 dose onto Pd(110) at 120 K resulted in the production of 0.26 ML of CO, the same as that for the nondeuterated case shown in Figure 1. However, an additional acetaldehyde desorption peak was observed at 252 K. The desorption behavior for acetaldehyde is very similar to that observed following acetaldehyde adsorption on Ru(001)[7] and Rh(111)[8] surfaces. Henderson et al.[7] attributed acetaldehyde desorption peaks at 250 and 310 K to the depolymerization of a physically adsorbed acetaldehyde polymer on Ru(001) rather than to reaction on the metal surface. On both Ru(001)[7] and Rh(111),[8] high-temperature acetaldehyde desorption states (above 200 K) were only observed after considerable filling of the multilayer state. However, no high-temperature desorption states due to acetaldehyde depolymerization were reported on the clean Ni(100)[5] and Pd(111)[4] surfaces, where acetaldehyde adsorption in the η^2 coordination was preferred. Interestingly, acetaldehyde oligomerization to paraldehyde on the sulfur-precovered Ni(100) surface[5] was observed where TPD results indicated a substantial presence of acetaldehyde in the η^1 coordination. Acetaldehyde TPD results in Figure 1 did not indicate any substantial high-temperature (> 200 K) acetaldehyde desorption after exposures large enough to produce a significant multilayer population, but nevertheless, there was evidence for acetaldehyde desorption taking place at ca. 250 K at all exposures (see Figure 2). It should be noted that the $m/e = 29$ signal, following a 1.0 L exposure of acetaldehyde (CH_3CHO) onto clean Pd(110) (see Figure 2), exhibited a peak at 160 K with a high-temperature shoulder at ca. 255 K. However, subsequent higher doses of acetaldehyde onto Pd(110) in Figure 2 did not show further growth of the high-temperature shoulder.

The methane product distributions from TPD experiments for high and low acetaldehyde-d_4 coverages on the clean Pd(110) surface at 120 K are shown in Figure 4a,b. There was significant hydrogen adsorption from the background (as high as 0.3 ML at times) in these studies. The distribution of methanes in Figure 4a resulting from decarbonylation of a saturated acetaldehyde-d_4 adlayer on Pd(110) (the corresponding CO product yield in TPD was ~0.26 ML) clearly indicated the release of methyl (CD_3) species on the surface. The amount of multihydrogenated methane was less than 10% of the total methane yield. The methane product distribution following a 0.4 L exposure of acetaldehyde-d_4 onto a "clean" Pd(110) surface is shown in Figure 4b, where the corresponding CO product yield in the TPD experiment was 0.075 ML. If one assumes that there was roughly one-quarter monolayer of hydrogen atoms preadsorbed from the background on Pd(110) prior to the acetaldehyde-d_4 exposure, the CD_3H to CD_4 ratio would be approximately 3:1, which was exactly the ratio in Figure 4b. There was a small amount of CD_2H_2 formation as well, indicating some H−D exchange.

In another set of experiments, acetaldehyde (CH_3CHO) was dosed onto a Pd(110) surface precovered with 1 ML of D atoms

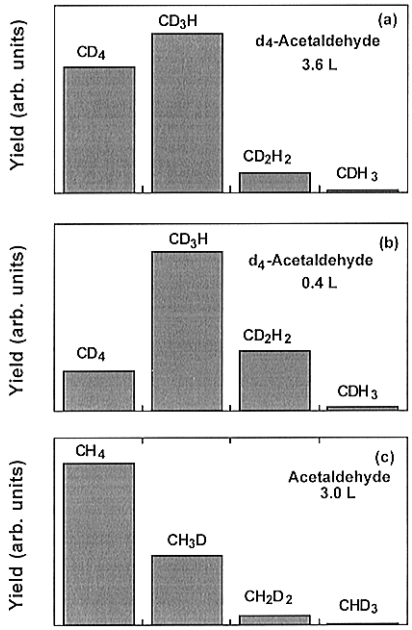

Figure 4. Distribution of methane produced following (a) 3.6 L exposure of CD_3CDO; (b) 0.4 L exposure of CD_3CDO onto the initially clean Pd(110) surface at 120 K; and (c) 3.0 L exposure of CH_3CHO on a 1 ML deuterium-precovered Pd(110) surface at 120 K.

at 120 K. The H/D ratio before the acetaldehyde dose was estimated to be 1:3.3 based on TPD experiments in which D_2 but not acetaldehyde was dosed. The large amount of deuterium present on the surface before acetaldehyde decarbonylation was expected to produce substantial deuteration in the methane product. The resulting methane product distribution following a 3 L exposure of acetaldehyde(CH_3CHO) on 1 ML D-precovered Pd(110) (the corresponding CO product yield in TPD was 0.18 ML) is shown in Figure 4c. Another experiment with low acetaldehyde exposure on a similarly prepared D-precovered Pd(110) surface, with a corresponding CO yield of 0.08 ML, reproduced the methane product distribution shown in Figure 4c. The extent of deuteration in the methane produced was less than that expected for the case of the methyl species release on a deuterium-rich surface. Still, the amount of multideuterated methane was less than 10% of the total methane yield, which argues against the possibility of the presence of methylene (CH_2) species on the surface following decarbonylation of the acetaldehyde adlayer.

To gain further insight, the adsorption and reaction of acetaldehyde on Pd(110) were also studied with HREELS. A HREEL spectrum collected at 120 K following a 4.2 L acetaldehyde exposure onto the clean Pd(110) surface at 150 K indicated multilayer acetaldehyde, η^2-acetaldehyde, and some acetyl species on the surface. The HREEL spectra following acetaldehyde adsorption on Pd(111) at 170 K[4] and on Pd(110) at 150 K in our study were in excellent agreement, except for the presence of one loss at 1724 cm^{-1} in the latter case. The mode at 1724 cm^{-1} in the spectrum shown in Figure 5 was attributed to the ν(CO) mode of acetaldehyde adsorbed in a condensed or physisorbed state.[20] The absence of this mode in the Pd(111) case[4] likely reflects the higher adsorption temperature employed in those studies. A similar mode at 1745 cm^{-1} was observed after acetaldehyde adsorption on Rh(111) at 90 K;[8] this peak disappeared upon heating the adlayer to 143 K. It should be noted that acetaldehyde on the clean Rh(111) surface desorbed from the physisorbed state at 140 K.[8] From vibrational studies of CH_3CHO and CD_3CDO on the clean Pd(111) surface at 170 K,[4] ν(CO) modes of two different adsorbed acetaldehyde

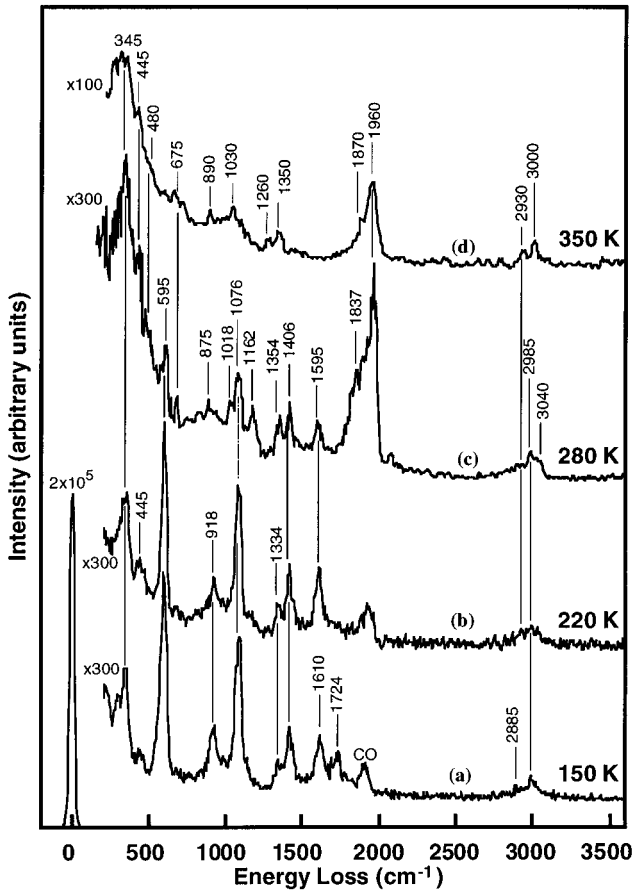

Figure 5. HREELS after an exposure of 4.2 L of acetaldehyde at 150 K and after subsequent annealing at indicated temperatures.

species were identified. The ν(CO) mode corresponding to acetyl ($CH_3C{=}O$) species, following the loss of the acyl hydrogen from η^2(C,O)-acetaldehyde, was observed at 1595 cm^{-1} and that of η^2(C,O)-acetaldehyde was at 1400 cm^{-1}. After conducting similar isotope-labeling HREELS studies, the losses due to the ν(CO) modes of η^2(C,O)-acetaldehyde on Ru(001)[7] and Rh(111)[8] have also been identified unambiguously at ca. 1380 and 1450 cm^{-1}, respectively. Due to interference with the methyl deformation modes of acetaldehyde, which are expected between 1380 and 1430 cm^{-1},[20] it was not possible to unambiguously identify the ν(CO) modes of η^2(C,O)-acetaldehyde in the present study. However, the asymmetric line shape of the loss at ca. 1406 cm^{-1} indicated the presence of the losses due to the ν(CO) modes and the methyl deformation modes of η^2(C,O)-acetaldehyde. Also, the asymmetry in the loss at 1406 cm^{-1} became more pronounced after heating the adlayer to 220 K. Comparison of HREEL spectra for CH_3CHO and CD_3CDO on Pd(111),[4] Ru(001),[7] and Rh(111)[8] indicated that losses due to methyl deformation modes of the acetaldehyde adlayer were at a lower frequency than those due to the ν(CO) modes of η^2(C,O)-acetaldehyde. On the basis of this observation, the loss at 1406 cm^{-1} is assigned predominantly to the ν(CO) modes of η^2(C,O)-acetaldehyde on Pd(110).

In Figure 5, the peak at 1610 cm^{-1} in the HREEL spectrum after acetaldehyde adsorption on Pd(110) at 150 K is assigned to the ν(CO) mode of acetyl adspecies. By comparison with organometallic platinum and palladium acetyl complexes,[21,22] ν(CO) modes for acetyl species from acetaldehyde reactions on Pt(S)-[6(111) × (100)][6] and Pd(111)[4] surfaces have been identified at 1650 and 1595 cm^{-1}, respectively. The losses due to the CO stretching mode of the acetyl ligand in the stable *trans*-[$PdBr(COCH_3)(PEt_3)_2$] complexes[22] range from 1661 to

TABLE 1: HREELS Vibrational Frequencies (cm^{-1}) and Mode Assignments of Acetaldehyde Adsorbed on Pd(110) at 150 K

mode description	crystalline IR[a]	Pd−acetyl $CH_3C{=}O$[b]	Pd(111) at 170 K[c]	Pd(110) at 150 K[d]
$\nu_a(CH_3)$	3003		2990	2985
	2964			
$\nu_s(CH_3)$	2918			
ν(CH)	2747		2850	2885
ν(CO)-acetyl		1667	1565	1610
ν(CO)-η^2	1722		1390	1406
$\delta(CH_3)$	1431	1324	1390	1334
$\delta_{as}(CH_3)$	1422			1334
δ(CH)	1389		1390	1334
$\delta_s(CH_3)$; ν(CH)	1347			nr[e]
$\rho(CH_3)$; ν(CC)	1118	1073	1080	1076
ρ(CH); $\rho(CH_3)$	1102			no[e]
ν(CC); $\rho(CH_3)$	882	903	900	918
ρ(CH); $\rho(CH_3)$	770			no[e]
δ(CCO)	522	571	600	595
ν(Pd−C)-acetyl			330	330, 445

[a] Reference 20. [b] Reference 22. [c] Reference 4. [d] This study. [e] nr = not resolved; no = not observed.

1675 cm^{-1} where the acetyl ligand is coordinated to the metal center via its unsaturated carbonyl carbon atom, i.e., in an η^1-(C) configuration. Due to the presence of a halide ligand in the above mononuclear palladium−acetyl complex, very little overlap between the metal d orbitals and the carbonyl π^* orbital is expected and hence, a higher CO stretching frequency is observed. Acetyl species on metal surfaces exhibit a greater degree of back-bonding, and lower CO stretch frequencies are observed in HREELS.[4,6] The lower coordination number of surface metal atoms on Pd(110), seven vs nine on Pd(111), should lead to weaker back-bonding as compared to Pd(111) and hence a somewhat higher CO stretching frequency for acetyl on Pd(110). Some background CO contamination was also observed in HREELS. The rest of the modes for the acetaldehyde adlayer on Pd(110), in congruence with the IR assignments of crystalline acetaldehyde[20] and previous HREELS assignments for acetaldehyde on the clean Pd(111) surface,[4] are compiled in Table 1.

There were no significant changes upon heating the acetaldehyde adlayer to 220 K, except for the disappearance of the 1724 cm^{-1} peak. Only η^2(C,O)-acetaldehyde and acetyl species were present on the surface at this temperature. When the acetaldehyde adlayer on Pd(110) was heated to 280 K, decarbonylation took place, as is evident from the ν(CO) mode at 1960 cm^{-1}. Similar losses after CO adsorption[23] and methanol decomposition[24] on the clean Pd(110) surface at 110 K have been reported, where CO was bound at 2-fold bridge sites. However, attenuated modes typical of η^2(C,O)-acetaldehyde and acetyl adspecies were still present at 280 K. It should be noted that the acetaldehyde adlayer on Pd(111)[4] was observed to be intact until 300 K. In the HREEL spectrum at 280 K in Figure 5, new modes at 480, 675, ~875, 1018, 1162, ~1350, and 3040 cm^{-1} were observed. The ν(CH) mode higher than 3000 cm^{-1} indicated the presence of hydrocarbon adspecies with sp^2 or sp carbon,[25] possibly due to methyl dehydrogenation products on the surface, e.g., methylene or methylidyne. The new modes could indicate a mixture of C_1 surface hydrocarbons.[26−29] The stretching mode of the metal−CH_x(ad) bond may also contribute to the intensity of the loss at 480 cm^{-1}. The evidence for methylene (CH_2) groups was limited, as the relative intensities expected for various modes of methylene adspecies on metal surfaces[28,29] were not observed. In particular, the most intense peak expected at ~930 cm^{-1} due to the CH_2 twist mode[28] is absent in Figure 5c. On the other hand, the deformation modes

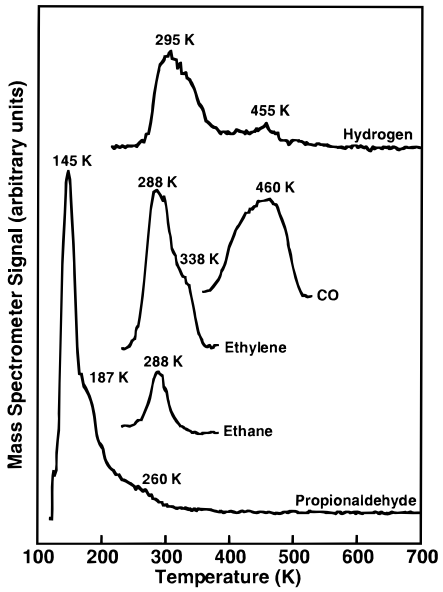

Figure 6. TPD spectra following a saturation exposure of propionaldehyde onto the initially clean Pd(110) surface at 120 K.

of the methyl group, namely, $\delta_a(CH_3)$ and $\delta_s(CH_3)$, could be seen distinctly at ca. 1354 and 1162 cm^{-1}. Little interference between methyl deformation modes due to acetyl/η^2(C,O)-acetaldehyde and those due to methyl adspecies would be expected. Nonetheless, the increased intensity ratio of the loss at 1334 cm^{-1} to that at 1406 cm^{-1} after annealing at 280 K, as compared with the corresponding ratio in the HREEL spectrum at lower temperature (before decarbonylation), suggested the presence of methyl species on the surface. However, it is to be noted that methyl species on clean Ni and Ru have previously been reported[26,27] to be unstable at 280 K, the temperature at which they appeared to be most prominent in the present study.

As noted above, some acetaldehyde and acetyl species persisted on the surface at 280 K. In previous detailed studies of the surface chemistry of ketene ($CH_2{=}C{=}O$) on Pt(111)[29] and Ru(001),[30] White and co-workers demonstrated that molecularly adsorbed ketene was hydrogenated below 250 K to produce adsorbed η^2(C,O)-acetaldehyde (CH_3CHO) and η^2(C,O)-acetyl (CH_3CO) species. It was further established that η^2-acetaldehyde decomposed at ca. 330 K, whereas the η^2-acetyl intermediate was stable until 440 K.[30] On the basis of extensive literature references for bridging η^2(C,O)-acetyl[31−38] and η^2-(C,O)-acyl[39−41] organometallic complexes, Henderson et al.[30] have assigned the prominent losses at 1425, 1160, 985, and 675 cm^{-1} in the HREEL spectrum after annealing the ketene adlayer on Ru(001) at 400 K to the ν(CO), ν(CC), $\rho(CH_3)$, and π(CCO) modes of η^2(C,O)-acetyl adspecies, respectively. Comparison of loss peaks in Figure 5c, especially the loss at ca. 675 cm^{-1} with those of Henderson et al.[30] noted above, does suggest the presence of some acetyl species in an η^2(C,O) configuration; however, the loss at 1595 cm^{-1} was assigned to η^1(C)-acetyl adspecies. After the adlayer was heated up to 350 K, the acetyl and acetaldehyde modes disappeared completely and the remaining modes were attributable to CO and C_1 hydrocarbon species on the surface. An important observation was the relative decrease in the loss intensity due to the ν(CO) stretching mode of the acetyl ligand in the HREEL spectrum at 350 K.

3.2. TPD and HREELS of Propionaldehyde on Pd(110) Surfaces. TPD spectra obtained following a greater-than-saturation exposure (3.6 L) of propionaldehyde onto the clean Pd(110) surface are shown in Figure 6. The TPD products were propionaldehyde, ethane (288 K), ethylene (288 and 338 K),

TABLE 2: Product Yields (ML) Following 3.6 L Exposure of Propionaldehyde onto an Initially Clean Pd(110) Surface at 120 K

products (desorption temp, K)	yield (ML)
CH_3CH_2CHO (145, 187 K)	0.5, 0.1
C_2H_4 (288, 338 K)	0.18
C_2H_6 (288 K)	0.06
H_2 (250−550 K)	0.43
CO (460 K)	0.32
C(ad)	0.17

CO (460 K), hydrogen, and surface carbon. No methane was observed. Hydrogen desorption took place with peaks at 295, 330, and 455 K and with a high-temperature tail persisting until 550 K. The low-temperature hydrogen evolution at 295 K was desorption-limited[18] and the high-temperature, reaction-limited hydrogen evolution was due to the decomposition of hydrocarbon adspecies following decarbonylation of the adsorbed propionaldehyde molecule. Recent studies by Nishijima et al.[42] of the decomposition of ethylene on Pd(110) have shown, based on HREELS and TPD results, that ethylene decomposes between 260 and 300 K to give ethynyl (CCH) species, hydrogen adatoms, and unstable vinyl ($CH{=}CH_2$) species. The ethynyl species produced from ethylene decomposition on Pd(110)[42] dehydrogenated completely to release hydrogen in the temperature range 450−520 K and deposit surface carbon. The hydrogen desorption signature following propionaldehyde reactions on Pd(110), shown in Figure 6, was similar to those after ethylene decomposition on Pd(110) reported by Nishijima et al.[42] The CO evolution at 460 K in Figure 6 was desorption-limited.[19] The CO desorption following propionaldehyde decomposition in Figure 6, unlike its characteristic first-order desorption from clean Pd(110),[19] took place over a broad temperature range of 350−500 K. However, CO desorption from hydrocarbon-containing Rh(111) surfaces[43,44] has also been found to be broadened on the lower-temperature side of the peak relative to its characteristic first-order desorption from the clean surface, and similar behavior was also observed for desorption of CO following decarbonylation of allyl alcohol and acrolein on Pd(110).[13]

The yields of the reaction products in Figure 6 are presented in Table 2. The amount of surface carbon deposited from the propionaldehyde decomposition was determined in subsequent oxygen TPD experiments by integration of the CO_2 and CO desorption peaks from burnoff reactions of surface carbon. The different desorption states of propionaldehyde following its adsorption on the clean Pd(110) surface at increasing exposures are shown in Figure 7. Propionaldehyde desorption was identified by monitoring $m/e = 58$ with the mass spectrometer during TPD experiments. Following propionaldehyde adsorption on Pd(110) at 120 K, the parent molecule desorbed mainly from two states. The low-temperature desorption peak at 145 K was attributed to propionaldehyde desorption from a multilayer or condensed state, whereas the peak at 187 K was assigned to propionaldehyde desorption from the monolayer state chemisorbed in an η^1 configuration. A small amount of propionaldehyde desorption as a high-temperature shoulder ca. 250 K was always observed, without any significant growth with increasing exposures. In an earlier study of propionaldehyde adsorption on the clean Pd(111) surface at 170 K,[4] propionaldehyde desorption states at 200 and 325 K were observed; the high-temperature desorption peak at 325 K was assigned to the desorption of propionaldehyde adsorbed in an η^2(C,O) configuration on Pd(111).[4] No such high-temperature propionaldehyde desorption peak was observed in our studies as shown in Figure 7.

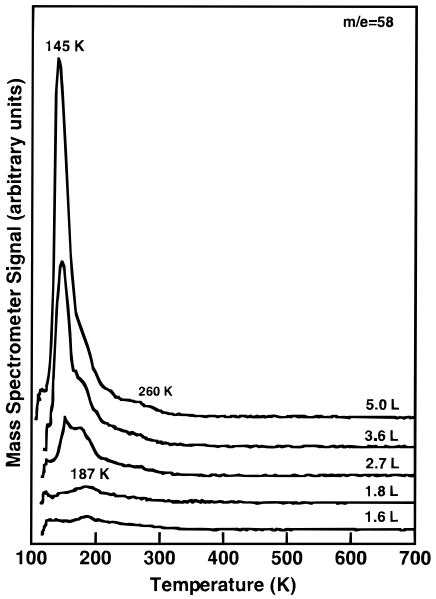

Figure 7. Series of $m/e = 58$ spectra following indicated exposures of propionaldehyde onto the initially clean Pd(110) surface at 120 K.

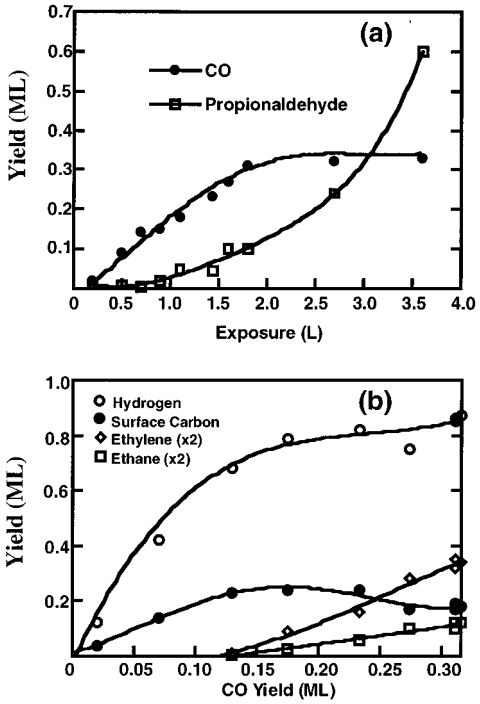

Figure 8. (a) Propionaldehyde decomposition (in terms of CO yield in TPD) and desorption yields for various exposures of propionaldehyde; (b) TPD product yields vs CO yield following propionaldehyde TPD.

The coverage-variation studies for propionaldehyde adsorption and reaction on Pd(110) are summarized in Figure 8. The competition between propionaldehyde desorption and decomposition is reflected in Figure 8a. The saturation extent of propionaldehyde decomposition, represented in terms of CO yield (ML), was attained by a 1.8 L exposure of the parent molecule. Negligible propionaldehyde desorption took place until 0.9 L exposure. Then, propionaldehyde desorbed at 187 K from the chemisorbed state, while the CO product yield continued to increase. For exposures greater than 1.8 L, no enhancement in the CO product yield was observed, and propionaldehyde desorption from the multilayer state at ca. 145 K continued to increase. Figure 8b illustrates two competing pathways for the propionaldehyde reaction on the Pd(110) surface. At low coverages, adsorbed propionaldehyde decom-

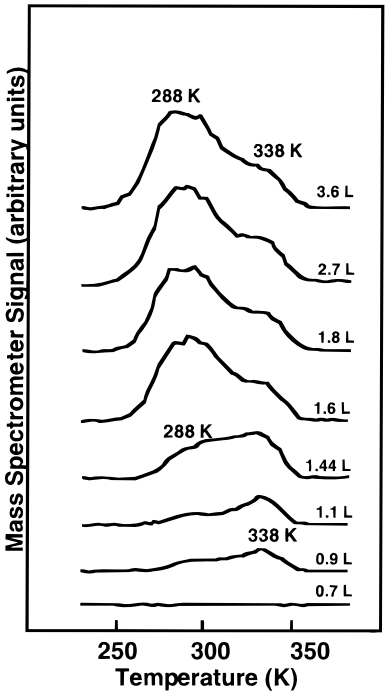

Figure 9. TPD spectra of ethylene produced following decarbonylation after indicated exposures of propionaldehyde onto the initially clean Pd(110) surface.

posed unselectively to release H_2 and CO and to deposit surface carbon. However, hydrocarbon evolution took place past 0.15 ML CO yield. Desorption of hydrocarbons one atom shorter than the parent molecule, following propionaldehyde reactions on Pd(111)[4] and Rh(111),[9] has been observed previously. Propionaldehyde adsorbed on the clean Pd(111) surface at 170 K[4] underwent decarbonylation to release CO, H_2, ethylene, and surface carbon, whereas that on the clean Rh(111) surface at 91 K[9] produced CO, H_2, ethane, and surface carbon. The production of a hydrocarbon one atom shorter than acetaldehyde has previously been noted for acetaldehyde reactions on Pd(110), Pd(111),[4] Ru(001),[7] and Rh(111).[8] In the case of propionaldehyde decarbonylation on Pd(110), two ethylene product desorption states were identified, as shown in Figure 9. Ethylene desorption at 338 K initially grew in parallel with the low-temperature desorption state at ca. 288 K. With increasing propionaldehyde decarbonylation on Pd(110) as shown in Figure 8(a), more ethylene desorption took place at 288 K than at 338 K. The relative ratio of ethylene desorption at the two temperatures (low to high) was 2:1 at saturation coverage. A similar reaction-limited ethylene desorption signature following decomposition of a saturated propionaldehyde layer on Pd(111)[4] has been reported. In studies of ethylene reactions on the clean Pd(110) surface,[42] ethylene decomposed unselectively to hydrogen and surface carbon at low coverages, and then, at increased coverage, desorbed at 300 K via the recombination of hydrogen adatoms and vinyl ($CH{=}CH_2$) adspecies. Desorption of physisorbed (π-bonded) ethylene from the clean Pd(110) surface[42] was observed as a plateau between ~150 and 260 K.

Propionaldehyde adsorption and decarbonylation were investigated on a Pd(110) surface precovered with 1 ML of hydrogen. Two propionaldehyde coverage regimes were considered. The slate of TPD products following propionaldehyde reactions on the hydrogen-precovered Pd(110) surface and that on the initially clean Pd(110) remained the same. Most importantly, no aldehyde hydrogenation to the corresponding alcohol was observed. In both coverage regimes, propionaldehyde adsorption on the H-precovered Pd(110) surface increased as compared to the corresponding values on the clean Pd(110) surface. However, the presence of hydrogen on Pd(110) favored desorption of the parent molecule over decarbonylation. In a similar fashion, the relative yield of ethane increased. The enhancement in ethane yield at the cost of reduced ethylene production was observed in this experiment where less ethylene desorption took place at ca. 290 K as compared with the corresponding propionaldehyde coverage on the clean Pd(110) surface. Nevertheless, the relative amount of total hydrocarbon in TPD experiments increased on the H-precovered surface. In the subsaturation coverage regime, the selectivity of hydrocarbon production, for comparable extents of propionaldehyde decomposition, increased nearly 6-fold on the H-precovered surface. The coverage-dependent hydrocarbon selectivity following propionaldehyde decomposition on Pd(110) as identified in Figure 8b was altered significantly by precovering the Pd(110) surface with hydrogen adatoms in the subsaturation regime as shown in Table 3. Also, the propionaldehyde desorption vs decarbonylation ratio was altered for comparable propionaldehyde coverages on the hydrogen-precovered Pd(110) surface. Previous propionaldehyde/hydrogen codose experiments on Rh(111) surface[9] also led to similar conclusions.

TABLE 3: Propionaldehyde Reactions on 1 ML Hydrogen−Precovered Pd(110) Surfaces

	subsaturation regime		near-saturation regime	
hydrogen exposure (L)	0.0	0.3	0.0	0.3
propionaldehyde exposure (L)	0.9	0.8	1.8	1.8
H_2 yield (ML)	0.34	0.76	0.42	0.80
CO yield (ML)	0.13	0.16	0.31	0.27
C_2H_4 yield (ML)	0.005	0.03	0.16	0.12
C_2H_6 Yield (ML)	0.002	0.02	0.05	0.08
propionaldehyde yield (ML)	0.02	0.04	0.10	0.19

Further insight into propionaldehyde chemistry on Pd(110) was obtained by experiments involving a 1.8 L exposure of propionaldehyde onto a 1 ML deuterium-precovered Pd(110) surface. TPD spectra corresponding to various *m*/*e* ratios are shown in Figures 10 and 11. After accounting for the natural abundance of carbon ^{13}C isotope (~1.34%) in the parent molecule (CH_3CH_2CHO) and subsequent deconvolution, the TPD spectrum for $m/e = 59$ was assigned to the evolution of monodeuterated propionaldehyde at ca. 255 K (indicated by the shaded area). However, the nature of the mechanism leading to monodeuterated propionaldehyde desorption at 255 K is not clear. No previous suggestion for aldehyde desorption after acyl and hydrogen adspecies recombination exists in the literature. Nevertheless, an acetaldehyde desorption peak at 255 K due to depolymerization of acetaldehyde oligomers on Pd(110) was observed earlier. A small amount of propionaldehyde desorption as a high-temperature shoulder at ca. 255 K was also observed, as shown in Figure 6. It is speculated that propionaldehyde desorption at ca. 255 K also results from similar depolymerization reactions of the aldehyde oligomer. Fragmentation of the oligomer may produce acyl as well as aldehyde species; reaction of these acyls with surface D atoms would produce the deuterated aldehyde.

A portion of the ethylene produced at high temperature (338 K) was completely deuterated on a deuterium-precovered Pd(110) surface, as is evident from the $m/e = 32$ desorption peak at 338 K in Figure 11. Likewise, the formation of traces of completely deuterated ethane was also apparent from the $m/e = 36$ spectrum. The production of both multideuterated ethylene and ethane at ca. 290 K took place following

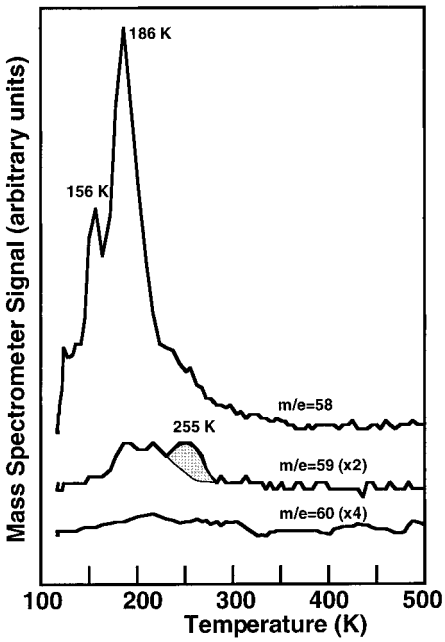

Figure 10. TPD spectra for indicated *m*/*e* values following propionaldehyde dose (1.8 L) onto the initially clean Pd(110) surface precovered with 1 ML of deuterium. The shaded area corresponds to the signal from propionaldehyde-d_1 (see text).

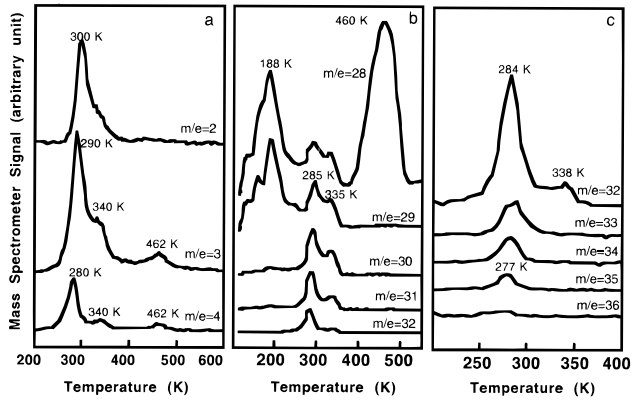

Figure 11. TPD spectra following propionaldehyde dose (1.8 L) onto a 1 ML deuterium-precovered Pd(110) surface (a) depicting *m*/*e* = 2−4; (b) depicting *m*/*e* = 28−32; (c) depicting *m*/*e* = 32−36.

propionaldehyde decarbonylation, as is evident from the *m*/*e* = 28−36 spectra in Figure 11. The mass fragment distribution (*m*/*e* = 26−36 peak areas) resulting from hydrocarbon evolution at ca. 290 K in the TPD experiment following 1.8 L exposure of propionaldehyde onto the D-precovered Pd(110) surface is shown in Figure 12a. The H:D ratio on the surface before propionaldehyde exposure was estimated to be 1:3.3. The presence of hydrogen on the surface was due to hydrogen adsorption from the chamber background during surface preparation. The H:D ratio from the TPD peak areas of *m*/*e* = 2, 3, and 4 in Figure 11, following propionaldehyde reactions on the deuterium-precovered Pd(110) surface, was nearly 1.3:1. Because of interfering mass fragments of various C_2 hydrocarbon products in Figure 12a, the deconvolution of individual product contributions was a challenging task. However, simulation of the mass fragment distribution for *m*/*e* = 26−36 was carried out by assuming complete random scrambling of deuterium in the ethylene and ethane products. In other words, this model assumes that the original hydrogens of the hydrocarbon species released on the surface by propionaldehyde decarbonylation underwent rapid exchange with the surface H/D pool. Only this type of modeling could provide all $d_i(i = 0-4)$-substituted

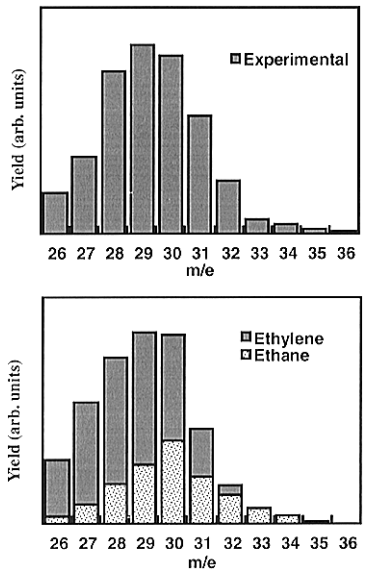

Figure 12. Mass fragment (*m*/*e* = 26 to *m*/*e* = 36 peak area) distribution (a) observed for the 1.8 L exposure of propionaldehyde onto the initially clean Pd(110) surface precovered with 1 ML of deuterium; (b) predicted from a random-scrambling model with H−D exchange (H:D = 1.25:1.0).

ethylenes and $d_i(i = 0-6)$-substituted ethanes, with individual distributions defined by the overall surface H/D ratio. The simulated mass fragmentation distribution, with a H/D ratio of 1.25:1 is shown in Figure 12b. The random scrambling model was found to be in much better agreement with the observed distribution than the models which permitted deuterium addition but no H−D exchange. The nonscrambling models prohibited formation of highly deuterated products, in disagreement with our experimental observation in Figure 12a. Again, the spectra depicting *m*/*e* = 2, 3, and 4 in Figure 11 showed very little evolution of reaction-limited hydrogen as compared with its isotopic counterpart. This observation of the larger amount of reaction-limited deuterium evolution in Figure 11 supports the conclusion that rapid isotope-scrambling takes place in the hydrocarbon fragments on the surface and explains the formation of the considerable amounts of multideuterated ethylenes apparent in Figure 12. A similar observation of vanishingly small amounts of reaction-limited deuterium and considerable hydrogen during ethylene (C_2D_4) decomposition on an H-precovered Pd(110) surface[45] was attributed to the prominence of the H−D exchange reaction. It should be noted that the simulation above required the following inputs: (1) the ratio of ethylene to ethane produced in a similar TPD experiment after propionaldehyde adsorption on 1 ML H-precovered Pd-(110) surface, (2) the H/D ratio of surface atoms available for addition or exchange with surface hydrocarbon species, and (3) the literature fragmentation patterns for $C_2H_xD_{4-x}$ ethylenes and $C_2H_xD_{6-x}$ ethanes.[46]

Following the successful simulation of the observed mass fragmentation distribution (see Figures 11 and 12), the resulting product distributions for the different hydrocarbon production channels were determined and are depicted in Figure 13. The deconvolution of ethylene products at 335 K was straightforward where the contributions due to mass fragments corresponding to ethylene-d_4 (*m*/*e* = 32) were subtracted from lower *m*/*e* ratios, and this procedure was continued for the next less-deuterated ethylene and so on. The product distribution of various ethylenes and ethanes at 285 K is based on the simulation of the observed mass fragmentation (*m*/*e* = 26−36) ratios, as discussed above. The ethylene produced at 335 and 285 K showed nearly the same isotopic distribution, with roughly 10%

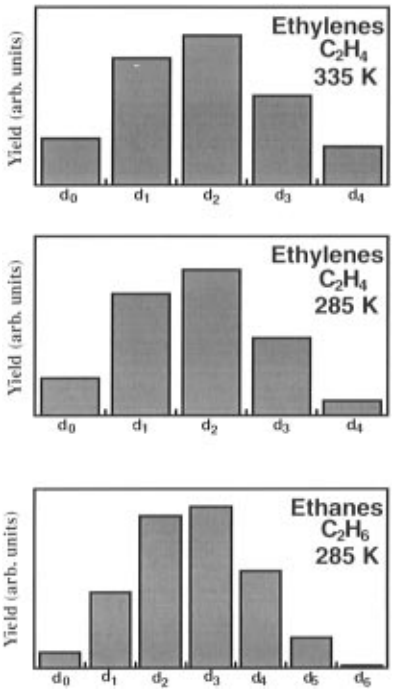

Figure 13. Deconvoluted TPD hydrocarbon product distribution following 1.8 L exposure of propionaldehyde onto the Pd(110) surface precovered with 1 ML of deuterium, at 120 K.

more deuteration in the ethylenes produced at higher temperature. However, a significant amount of the ethylene produced at 285 or 335 K contained one to two deuterium atoms. Similarly, the approximate ethane distribution emerging from our simulation of experimental results indicates substantial amounts of d_2- and d_3-substituted ethanes.

HREELS investigations of propionaldehyde on Pd(110) were carried out in order to identify the adsorption states and possible reaction intermediates. HREELS following a 3.6 L exposure of propionaldehyde onto clean Pd(110) at 140 K indicated, similar to acetaldehyde HREELS results, adsorption of propionaldehyde in two different coordinations, along with the presence of propanoyl ($CH_3CH_2C{=}O$) species. HREEL spectra following propionaldehyde adsorption on Pd(110) at 140 K and after annealing to higher temperatures are shown in Figure 14. The loss at 1685 cm^{-1} in the HREEL spectrum, shown in Figure 14a, indicated the presence of propionaldehyde in an η^1 coordination. Earlier HREELS experiments following propionaldehyde adsorption on Pd(111)[4] and Rh(111)[9] have reported molecular propionaldehyde adsorption in an η^1 coordination identified by losses at 1710 and 1700 cm^{-1}, respectively. The rest of the losses in Figure 14a compared favorably with the liquid-phase IR frequencies of propionaldehyde.[47] Specific vibrational mode assignments following propionaldehyde adsorption on clean Pd(110) at 140 K and on clean Pd(111)[4] and Rh(111)[9] surfaces along with literature reports of IR frequencies of liquid-phase propionaldehyde[47] are summarized in Table 4. As mentioned earlier for the acetaldehyde case, the ν(CO) mode for η^2(C,O)-propionaldehyde is expected to appear in a frequency range similar to that of the $\delta(CH_3)$ and $\delta(CH_2)$ modes of the aldehyde layer. Due to improved resolution of the HREEL spectrometer used in the present studies, it was possible to resolve many of these different modes for the first time, as compared with previous propionaldehyde adsorption studies on metal surfaces.[4,9] In the present study, a distinct loss at 1237 cm^{-1} was observed and is attributed to $\tau(CH_2)$ modes, based on a recent IR assignment of gas-phase propionaldehyde.[48] Another distinct loss at 980 cm^{-1}, as compared with previous

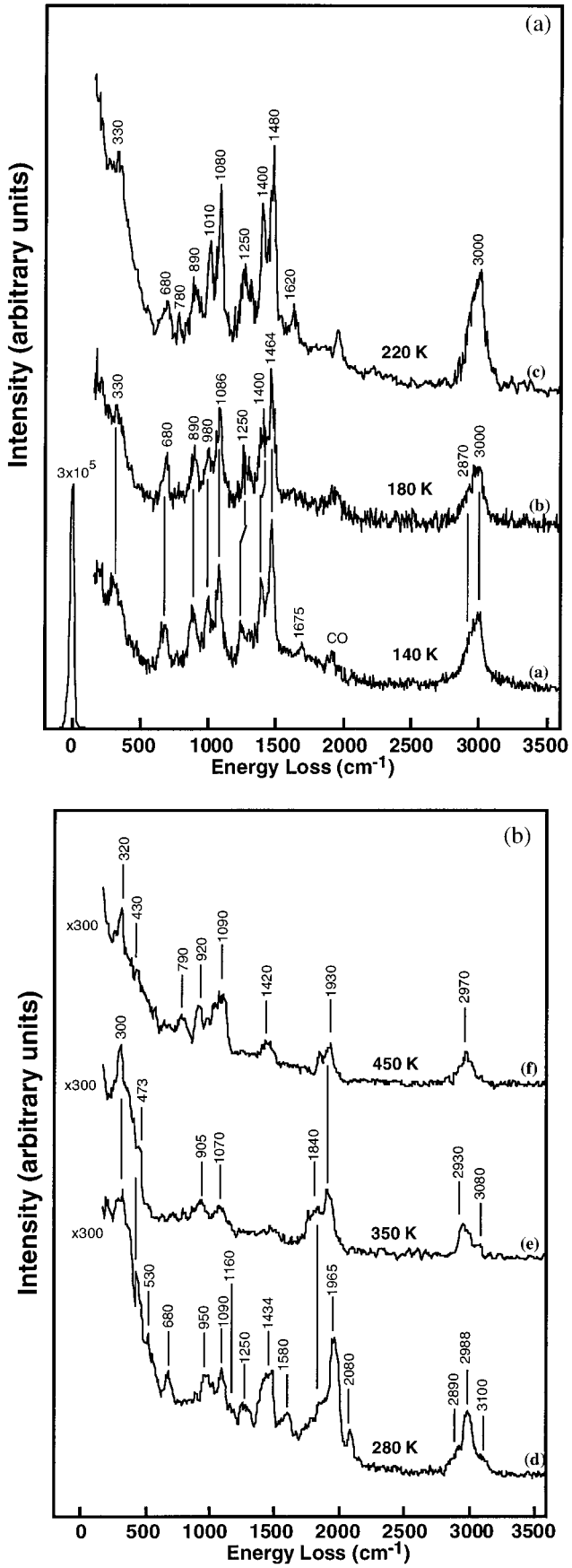

Figure 14. HREELS after an exposure of 3.6 L of propionaldehyde onto the initially clean Pd(110) surface at 150 K.

studies,[4,9] was assigned to the coupling of the methyl rocking $\rho(CH_3)$ mode and C−C stretching ν_s(CCC) mode. However, loss peaks due to the vibrational modes of hydrogen adsorbed

TABLE 4: HREELS Vibrational Frequencies (cm^{-1}) and Mode Assignments for the Adsorbed Propionaldehyde Layer on Metal Surfaces

mode	liquid IR[a]	Pd(111), 170 K[b]	Rh(111), 91 K[c]	Pd(110), 150 K[d]
$\nu(CH_3)$	2966	2950	2995	3000
$\nu(CH_2)$	2909	nr	2995	2870
ν(CO)-η^1-EtCHO	1730	1710	1700	1675
ν(CO)-(EtC═O)		1575		1620
$\delta(CH_2)$	1458	1400	1460	1464
$\delta(CH_3)$	1418	1400	1390	1373
ν(CO)−η^2EtCHO		1400		1464
$\tau(CH_2)$				1230
ν_a(CCC)	1092, 1120	1050	1110	1086
$\rho(CH_3)$	898	920	925	890
ν_s(CCC)		920		980
δ(CCO)	660	680	700	680
ν(Pd-C)-(EtC═O)		350		470, 330

[a] Reference 47. [b] Reference 4. [c] Reference 9. [d] This work. [e] nr = not resolved.

on the unreconstructed (1×1) Pd(110) surface also have been reported at ca. 770 and 950 cm^{-1},[49,50] introducing some ambiguity for this assignment.

Annealing the propionaldehyde adlayer on Pd(110) to 180 K resulted in severe attenuation of the ν(CO) stretching mode of η^1-propionaldehyde at 1685 cm^{-1} and the emergence of a new peak at 1620 cm^{-1} indicative of the presence of η^1(C)-propanoyl adspecies. Also, the loss at 1237 cm^{-1}, assigned to the $\tau(CH_2)$ mode, increased in intensity and shifted to 1250 cm^{-1}. The loss at 980 cm^{-1} was also attenuated as compared with the spectrum in Figure 14a which suggested that this loss indeed originated from the propionaldehyde adlayer and not from the vibrational modes of adsorbed hydrogen, as hydrogen does not desorb at such low temperatures. These subtle changes in Figure 14b indicated rearrangement of the propionaldehyde adlayer following desorption of the weakly adsorbed propionaldehyde, as observed earlier during TPD experiments.

Several changes took place after annealing the propionaldehyde adlayer to 220 K. The appearance of a sharp loss at 1620 cm^{-1}, indicating more propanoyl formation, was accompanied by broadening of the losses at ca. 680 and 1250 cm^{-1}. Furthermore, a new loss at 780 cm^{-1} appeared and the relative intensities of the losses at 680 and 890 cm^{-1} decreased, suggesting a change in orientation of the carbon (CCC) backbone of the adlayer. The loss at 780 cm^{-1} could be due to the vibrational modes of the hydrogen adsorbed on the surface following propionaldehyde (CH_3CH_2CHO) dehydrogenation to propanoyl (CH_3CH_2C═O) intermediates. The adlayer underwent complete decarbonylation upon annealing at 280 K, as is evident from the characteristic strong losses due to CO on Pd(110) in the range 1840−2080 cm^{-1}.[23,24] The CO stretching region, following CO adsorption on the clean Pd(110) surface at 110 K,[23] is dominated by one band shifting from 1890 to 2000 cm^{-1} with increasing coverage and is assigned to CO adsorbed in 2-fold sites. A small loss due to CO adsorbed at on-top sites on Pd(110) was also observed at ca. 2100 cm^{-1} only after reaching 1 ML CO coverage on this surface.[23] The small loss at 2080 cm^{-1} in Figure 14d is indicative of a small amount of CO adsorbed at on-top sites. It is plausible that CO in the presence of the adsorbed hydrocarbons and hydrogen atoms released by decarbonylation of the propanoyl adspecies on the surface is pushed into on-top sites on Pd(110). This observation explains the broad CO desorption peak shape during propionaldehyde TPD experiments, discussed earlier. In the HREEL spectrum in Figure 14d, a completely new set of losses at ∼3100, 2988, 1580, ∼1434, 1280, 1080, 950, 650, ∼500, ∼420, and 300 cm^{-1} was observed. The losses due to various modes of η^2(C,O)-propionaldehyde and propanoyl disappeared completely. The observation of CH stretching modes above 3000 cm^{-1} indicated the presence of hydrocarbon species on the surface containing sp^2 or sp hybridized carbon.[25] Furthermore, the loss at 1580 cm^{-1} could be attributed to the stretching modes of the C═C group. The losses at 1434 cm^{-1} are too high in frequency to be due to methyl deformation modes and are thus assigned to $\delta(CH_2)$ modes. The similarity of losses in our study in the range 600−1600 cm^{-1}, following annealing of the propionaldehyde adlayer at 280 K, suggests the presence of a vinyl (CH_2CH) intermediate. There are few studies of vinyl intermediates on the metal surfaces, e.g., on Ni(100)[51] and Pt(111).[52] In a study of ethylene decomposition on clean Pd(110),[42] no evidence for vinyl species was observed; however, ethylene formation at 300 K following ethylene adsorption on Pd(110) at low temperature was suggested to proceed via hydrogenation of a vinyl intermediate. Recently, Liu et al.,[52] after studying vinyl iodide chemistry on Pt(111) surfaces, have reported that vinyl adspecies could be stabilized up to 450 K in the presence of iodine.

HREELS following annealing of the adlayer to higher temperatures, 350 and 450 K, indicated the presence of hydrocarbons and CO on the surface. The loss intensity due to the CO stretching mode at ca. 1900 cm^{-1} in the HREEL spectrum shown in Figure 14e was attenuated substantially, even when no CO desorption was observed in TPD experiments at this temperature. This loss of intensity due to the ν(CO) mode could result from tilting of the C−Pd axis of CO in the presence of hydrocarbon residues on the surface. Tilting of CO adsorbed on Pd(110) has been observed previously by Chesters et al.[23]

4. Discussion

HREELS experiments following acetaldehyde and propionaldehyde adsorption on clean Pd(110) at low temperatures indicate that both aldehydes adsorb intact in two coordination states and react partially to form the corresponding acyls. Aldehyde adsorption in η^1(O) and η^2(C,O) configurations has also been reported on Pd(111),[4] Rh(111),[8,9] Ru(001),[7] and Pt(S)[6(111)×(100)][6] surfaces, with the η^1(O) mode stable only at low temperatures. Recent semiempirical extended Hückel calculations[53,54] for different adsorption geometries of formaldehyde and acetaldehyde on Pt(111), Pt(110), and stepped Pt(111) surfaces also suggest that the preferred adsorption geometry is the η^2 configuration. In the HREELS experiments, the loss due to the CO stretching mode of acyl intermediates on both Pd(111)[4] and Pd(110) surfaces persisted until ca. 280 K and indicated that the acyl is adsorbed in an η^1(C) configuration. However, some evidence for η^2(C,O)-acetyl adspecies on Pd(110) was also observed in HREELS (see Figure 5c) after annealing the acetaldehyde adlayer on Pd(110) at 280 K. Comparisons of the CO stretch modes of the acyl adspecies formed below 220 K, following acetaldehyde or propionaldehyde adsorption on Pd(111)[4] and Pd(110), suggest slightly weaker acyl−surface bonding on the (110) plane of palladium. Losses due to the ν(CO) mode of η^1(C)-acetyl on Pd(110) and Pd(111)[4] surfaces were observed at 1611 and 1565 cm^{-1}, respectively. Similar variations in losses due to the ν(CO) mode of η^1(C)-propanoyl on Pd(110) and Pd(111), 1620 vs 1595 cm^{-1}, were also observed. The lower coordination number of surface metal atoms on Pd(110) as compared with those on Pd(111) would lead to a lower degree of back-bonding to the carbonyl π^* orbital of the acyl. Due to the lack of sufficient resolution in previous HREELS studies of acetaldehyde on Pd(111),[4] it is not possible to compare the relative strength of η^2(C,O)-aldehyde

binding with the palladium surfaces. However, the results from TPD studies of acetaldehyde reactions on Pd(111)[4] and (110) surfaces provide insight into the relative stability of η^2(C,O)-aldehyde adspecies. Unlike aldehydes on Pd(111),[4] no high-temperature (>250 K) aldehyde desorption was observed in TPD experiments for either aldehyde on Pd(110). The absence of aldehyde desorption from the η^2 state on Pd(110) and the corresponding higher decarbonylation activity on the (110) plane than that on the (111) plane of palladium suggest that η^2-aldehydes exhibit a greater tendency to decompose on Pd(110) than on Pd(111). Delbecq and Sautet[54] have recently reported that the most common adsorption modes of formaldehyde and acetaldehyde on (111), (110), and stepped (111) surfaces of platinum were η^2(C,O). Their interpretation of results from extended Hückel calculations for aldehydes on Pt surfaces[54] was based on the analysis of the stabilizing two-electron and the destabilizing four-electron adsorbate−surface interaction. In comparison to Pt(111), lower coordination of the surface metal atoms on Pt(110) strongly reduces the destabilizing four-electron repulsion, leading to stronger bonding of aldehydes in the η^2 state.[54] These authors have further noted that the influence of the surface metal coordination number in the case of η^1(O)-aldehyde adsorption is relatively minor. Similar analogies to the above theoretical studies on Pt surfaces can be applied to explain the absence of aldehyde desorption from the η^2 state on Pd(110), as compared to previous observations of η^2(C,O)-aldehyde desorption from the Pd(111) surface.[4]

Acetaldehyde adsorbed on Pd(110) in the η^2 configuration underwent dehydrogenation to produce stable acetyls. The acetyls then decarbonylated at ca. 280 K to release CO, hydrogen atoms, and a C_1 hydrocarbon species on the surface. Isotopic labeling experiments clearly showed evidence for methyl release following decarbonylation of acetyls. No significant difference in the position or magnitude of methane desorption peaks due to acetaldehyde-d_0 or acetaldehyde-d_4 decarbonylation was observed, indicating the absence of any kinetic isotope effect. This observation suggests that C−C scission preceded C−H scission for the acetyl intermediates on Pd(110). A similar observation was made during acetaldehyde decomposition on the Rh(111) surface.[8] However, our observation of acetaldehyde decarbonylation on Pd(110) is in contrast with the previous study of acetaldehyde decomposition on the clean Pd(111) surface[4] where acetyl decomposition was inferred (on the basis of a kinetic isotope effect in temperature-programmed HREELS experiments) to proceed via removal of a hydrogen from the methyl group followed by C−C scission, releasing methylene species on the surface. Surprisingly, a very high selectivity for hydrogenation of surface methylene to produce methane was reported, and no methylene coupling reactions to form C_2 hydrocarbons were observed. While TPD experiments following acetaldehyde-d_4 adsorption on hydrogen-precovered Pd(110) indicated the expected methane product distribution, supporting the precedence of C−C scission over C−H scission in acetyl adspecies, acetaldehyde (CH_3CHO) decarbonylation on D-precovered Pd(110) did not give such a clear indication. The complexity of the HREEL spectrum in Figure 5c, after annealing the acetaldehyde adlayer at 280 K and subsequent decarbonylation, does not allow one to identify the methyl adspecies unequivocally. While intense losses observed at 1160 and 1350 cm^{-1} could be assigned to vibrational modes of methyl groups on the surface, the loss intensity at ca. 675 cm^{-1} is suggestive of the backbone deformation modes of acetyl/aldehyde adsorbed in an η^2(C,O) configuration. A small fraction of the adsorbed methyl groups dehydrogenated further to deposit surface carbon and release hydrogen until ca. 400 K. On the basis of TPD and HREELS studies, the following bond activation sequence is proposed to occur during acetaldehyde reactions on Pd(110):

$$CH_3CHO(g) \rightarrow \eta^1(O)\text{-}CH_3CHO(ad)$$

$$\rightarrow \eta^2(C,O)\text{-}CH_3CHO(ad)$$

$$\rightarrow \eta^1(C)\text{-}CH_3CO(ad) + H(ad)$$

$$\eta^1(O)\text{-}CH_3CHO(ad) \rightarrow CH_3CHO(g)$$

$$\eta^1(O)\text{-}CH_3CHO(ad) \rightarrow \eta^2(C,O)\text{-}CH_3CHO(ad)$$

$$\eta^2(C,O)\text{-}CH_3CHO(ad) \rightarrow \eta^1(C)\text{-}CH_3CO(ad) + H(ad)$$

$$\eta^1(C)\text{-}CH_3CO(ad) \rightarrow CH_3(ad) + CO(ad)$$

$$CH_3(ad) + H(ad) \rightarrow CH_4(g)$$

$$CH_3(ad) \rightarrow C(ad) + 3H(ad)$$

$$2H(ad) \rightarrow H_2(g)$$

$$CO(ad) \rightarrow CO(g)$$

Overall, the mechanistic understanding emerging from the present work examining acetaldehyde decomposition on Pd(110) differs from similar studies on Pd(111).[4] First, no η^2-(C,O)-acetaldehyde desorption from the Pd(110) surface was observed, as compared to acetaldehyde desorption at 325 K from clean Pd(111).[4] Second, stronger evidence for the release of methyl adspecies after decarbonylation of the aldehyde adlayer on Pd(110) is noted here. However, this apparent structure sensitivity of acetaldehyde reaction on Pd(111) and Pd(110) surfaces can be understood further only by performing detailed electronic structure calculations of the metal−adsorbate complex.

Propionaldehyde adsorbed on the Pd(110) surface, similar to its C_2 analogue, reacted to produce CO, hydrogen, and C_2 hydrocarbon species on the surface. The absence of C_1 hydrocarbon evolution indicates that selective decarbonylation took place, thus releasing C_2 hydrocarbon fragments. No C_1 hydrocarbon formation during propionaldehyde decomposition has been reported on either Pd(111)[4] or Rh(111).[9] The adsorbed propionaldehyde on Pd(110), like that on Pd(111),[4] reacted with the metal surface via propanoyl formation; this intermediate underwent decarbonylation to produce various products in TPD experiments. Stoichiometric release of CO following propionaldehyde decomposition on Pd(111)[4] and Pd(110) was observed. The decarbonylation pathways of propanoyl intermediates on Pd(110) were observed to be coverage-dependent. At low coverages, adsorbed propionaldehyde decomposed unselectively to produce CO, hydrogen, and surface carbon. Previously, desorption of adsorbed ethylene on the clean Pd(110) surface[42] had been reported to be coverage-dependent. It is plausible that the C_2 hydrocarbon fragments released following decarbonylation of propanoyl intermediates dehydrogenated completely to release hydrogen and deposit surface carbon. With increasing coverages of propionaldehyde on Pd(110), a competition between desorption and decomposition of the adsorbed propionaldehyde was observed. Also, competitive dehydrogenation and desorption pathways of hydrocarbon fragments were

observed with increasing propionaldehyde decomposition. The presence of hydrogen on the Pd(110) surface before propionaldehyde exposure influenced these competitive pathways considerably, suggesting that hydrocarbon production is governed by the presence of hydrogen adatoms as well.

From acetaldehyde and propionaldehyde studies on Pd(111),[4] it was concluded that C−H cleavage is rate-determining for decarbonylation of acyl intermediates. As discussed above, acetaldehyde decomposition and acetyl decarbonylation on Pd(110) seem to conflict with the observations made on Pd(111).[4] HREELS following annealing of the saturated propionaldehyde adlayer on Pd(110) at 280 K indicated complete decarbonylation and, hence, the presence of C_2 hydrocarbon fragments and hydrogen on the surface. It is not possible to suggest the precedence of C−C scission over C−H scission in propanoyl decomposition with the help of isotope-labeling experiments alone, as described earlier. However, the nature of the hydrocarbon fragment released following propanoyl decarbonylation was indeed elucidated by the isotope-labeling experiments. At very low exposures of propionaldehyde, ethylene desorbed mainly at 338 K. If C−H scission occurred before decarbonylation of propanoyl on Pd(110) to release a hydrocarbon less saturated than ethyl species on the surface, the ethylene production should not have been delayed until 338 K. Previously, following low-temperature adsorption of ethylene on the clean Pd(110) surface,[42] π-bonded ethylene desorbed molecularly between 150 and 260 K. The rest of the ethylene adsorbed on Pd(110) in di-σ mode reacted below 300 K, via unstable vinyl (CH_2═CH) intermediates, to form ethynyl (CCH) and hydrogen on the surface.[42] Isotope-labeling ethylene studies on Pd(110)[42,45] further suggested that ethylene desorption from Pd(110) surface at ca. 300 K resulted from the recombination of vinyl and hydrogen species on the surface. Two possible scenarios for ethylene desorption at 338 K at low exposure will be discussed here. It is plausible that propanoyl intermediates underwent C−H scission and then C−C scission to release ethylene on the surface; these ethylene intermediates were di-σ bonded and quickly decomposed to form vinyl adspecies which, in turn, remained stable until ca. 338 K. However, it is hard to imagine vinyl adspecies being so stable, especially in the presence of significant amounts of hydrogen on the surface. Another scenario could be the release of ethyl adspecies after propanoyl decarbonylation where ethyl decomposed further to produce ethylene. It has previously been reported[45,52,55,56] that the rate of ethane formation is limited by the rate of ethyl recombination with hydrogen adatoms. In ethylene H−D exchange studies on Pd(110)[45] and Pt(111)[52,56] surfaces, multideuterated ethane products have been observed. At saturation, ethylene desorption peaks at ca. 285 and 335 K were observed. Furthermore, propionaldehyde decomposition on the H-precovered Pd(110) surface resulted in more ethane evolution at 288 K, at the expense of ethylene at 288 K. The pronounced effect of hydrogen precoverage on ethane formation during propionaldehyde decomposition on Pd(110) suggests that the propanoyl intermediate decarbonylates first to release ethyl fragments on the surface. In previous TPD and HREELS studies of ethyl fragments on Pt(111) surface,[55] Lloyd et al. noted that ethyl fragments produced a mixture of π-bonded and di-σ bonded ethylenes and also a little ethane and ethylene desorbed from the π-bonded state. The di-σ bonded ethylenes dehydrogenated to ethylidynes which ultimately decomposed unselectively to produce hydrogen and deposit surface carbon.[55]

Previous studies of propionaldehyde reactions on Group VIII metal surfaces,[4,9] unlike the present study where *both* ethylene and ethane were observed, reported either ethylene *or* ethane formation. During propionaldehyde surface reactions, only ethylene from Pd(111)[4] and ethane from Rh(111)[9] were reported. When 1.2 L of deuterium and 1.58 L of propionaldehyde were codosed on the Rh(111) surface at 93 K,[9] d_i(i=0−6)-substituted ethanes were observed where the ethane product distribution indicated a *minimum* for the ethane-d_3 product yield. Random scrambling of H and D adatoms, for C_2(ad) and a H to D ratio of 1:1 in the above study, would predict a *maximum* for ethane-d_3 production, in contrast with the experimental observation on Rh(111).[9] The authors[9] proposed that ethyl fragments were released following propionaldehyde or propanoyl decarbonylation on the Rh(111) surface and considerable but nonrandom deuterium exchange took place to produce perdeuterioethane. A study of ethylene reactions on deuterium-precovered Pt(111) surface by Godbey et al.[56] also reported the formation of all possible deuterated ethanes, with a significant yield of ethane-d_6 during TPD. Godbey et al.[56] explained this observation by suggesting rapid equilibrium between adsorbed ethylenes and ethyl adspecies with further hydrogenation of ethyl species being the rate-limiting step for ethane formation. Recent studies of the C_2D_4 reaction on the H-precovered Pd(110) surface by Sekitani et al.[45] reported that the H−D exchange reaction (to form C_2D_3H) occurred predominantly via the ethyl species and only $C_2D_4H_2$, C_2D_5H, and C_2D_6 ethanes were observed. However, H−D exchange of ethylene on the clean Pd(110) surface to produce volatile ethylene and ethane[42] occurred via vinyl formation. In a study of vinyl surface chemistry on deuterium-precovered Pt(111),[52] Liu et al. have noted facile hydrogenation of vinyl to ethyl, leading to perdeuterioethane desorption. Overall, propionaldehyde results on clean and hydrogen- and deuterium-precovered Pd(110) surfaces indicate a coverage-dependent interplay of different factors, including (i) stability of ethyl fragments, (ii) availability of hydrogen adatoms, (iii) decomposition of ethyl to differently adsorbed ethylenes, and (iv) rapid equilibrium between vinyl and ethyl adspecies. However, unlike the acetaldehyde case, it is not feasible to suggest the clear precedence of C−C scission over C−H scission during propanoyl decomposition on Pd(110) surfaces.

5. Conclusions

Aldehyde reactions on Pd(110) and Pd(111) surfaces were determined to be structure-sensitive. No η^2(C,O)-aldehyde desorption from Pd(110) was observed, in contrast to previous studies on Pd(111). Isotope-labeling studies of aldehydes on Pd(110) suggest that the corresponding acyls decarbonylate to release alkyl fragments one carbon atom shorter than the probe reagent on the surface. In other words, C−C scission precedes C−H scission during acyl decomposition on Pd(110), in contrast to Pd(111) where this sequence is reversed. Detailed coverage-variation studies on clean and hydrogen- and deuterium-containing single-crystal surfaces provide important insights into the various competitive reaction pathways.

Acknowledgment. We gratefully acknowledge the support of the U.S. Department of Energy, Office of Basic Energy Sciences, Division of Chemical Sciences (Grant FG0284ER13290), for this research.

References and Notes

(1) Bell, A. T. *Catal. Rev.—Sci. Eng.* **1981**, *23*, 203.
(2) Biloen, P.; Sachtler, W. M. H. *Adv. Catal.* **1981**, *30*, 165.
(3) Ponec, V. *Catalysis* (London) **1981**, *5*, 48.
(4) Davis, J. L.; Barteau, M. A. *J. Am. Chem. Soc.* **1989**, *111*, 1782.
(5) Madix, R. J.; Yamada, T.; Johnson, S. W. *Appl. Surf. Sci.* **1984**, *19*, 43.

(6) McCabe, R. W.; DiMaggio, C. L.; Madix, R. J. *J. Phys. Chem.* **1985**, *89*, 854.
(7) Henderson, M. A.; Zhou, Y.; White, J. M. *J. Am. Chem. Soc.* **1989**, *111*, 1, 1185.
(8) Houtman, C. J.; Barteau, M. A. *J. Catal.* **1991**, *130*, 528.
(9) Brown, N. F.; Barteau, M. A. *Langmuir* **1992**, *8*, 862.
(10) Favre, T. L. F.; van der Lee, G.; Ponec, V. *J. Chem. Soc., Chem. Commun.* **1985**, 230.
(11) van der Lee, G.; Ponec, V. *Catal. Rev.—Sci. Eng* **1987**, *29*, 183.
(12) Clarke, J. K. A.; Rooney, J. J. *Adv. Catal.* **1976**, *25*, 125.
(13) Shekhar, R.; Barteau, M. A. *Surf. Sci.* **1994**, *319*, 298.
(14) Shekhar, R.; Barteau, M. A. *Catal. Lett.* **1995**, *31*, 221.
(15) Shekhar, R.; Barteau, M. A. *Surf. Sci.* **1996**, *348*, 55.
(16) Vohs, J. M.; Barteau, M. A. *Surf. Sci.* **1986**, *176*, 91.
(17) Plank, R. V.; DiNardo, N. J.; Vohs, J. M. *Surf. Sci.* **1995**, *340*, L971.
(18) Cattania, M. G.; Penka, V. Behm, R. J.; Christmann, K.; Ertl, G. *Surf. Sci.* **1983**, *126*, 382.
(19) Goschinck, J.; Grunze, M.; Loboda-Cackovic, J.; Block, J. H. *Surf. Sci.* **1987**, *189/190*, 137.
(20) Hollenstein, H.; Günthard, H. H. *Spectrochim. Acta A* **1971**, *27*, 2027.
(21) Dent, S. P.; Eaborn, C.; Pidcock, A.; Ratcliff, B. *Organomet. Chem.* **1972**, *46*, C68.
(22) Adams, D. M.; Booth, G. *J. Chem. Soc.* **1962**, 1112.
(23) Chesters, M. A.; McDougall, G. S.; Pemble, M. E.; Sheppard, N. *Surf. Sci.* **1985**, *164*, 425.
(24) Bhattacharya, A. K.; Chesters, M. A.; Pemble, M. E.; Sheppard, N. *Surf. Sci.* **1988**, *206*, L845.
(25) Biener, J.; Schenk, A.; Winter, B.; Lutterloh, C.; Schubert, U. A.; Küppers, J. *Surf. Sci.* **1994**, *307−309*, 228.
(26) Lee, M. B.; Yang, Q. Y.; Ceyer, S. T. *J. Chem. Phys.* **1987**, *87*, 2724.
(27) Zhou, Y.; Henderson, M. A.; Feng, W. M.; White, J. M. *Surf. Sci.* **1989**, *224*, 386.
(28) McBreen, P. H.; Erley, W.; Ibach, H. *Surf. Sci.* **1984**, *148*, 292.
(29) Mitchell, G. E.; Radloff, P. L.; Greenlief, C. M.; Henderson, M. A.; White, J. M. *Surf. Sci.* **1987**, *183*, 403.
(30) Henderson, M. A.; Radloff, P. L.; White, J. M.; Mims, C. A. *J. Phys. Chem.* **1988**, *92*, 4111.
(31) Butts, S. B.; Holt, E. M.; Strauss, S. H.; Alcock, N. W.; Stimson, R. E.; Shriver, D. F. *J. Am. Chem. Soc.* **1979**, *101*, 5864.
(32) Longato, B.; Norton, J. R.; Huffman, J. C.; Marsella, J. A.; Caulton, K. G. *J. Am. Chem. Soc.* **1981**, *103*, 209.
(33) Marsella, J. A.; Huffman, J. C.; Caulton, K. G.; Longato, B.; Norton, J. R. *J. Am. Chem. Soc.* **1982**, *104*, 6360.
(34) Yu, Y.-F.; Gallucci, J.; Wojcicki, A. *J. Am. Chem. Soc.* **1983**, *105*, 4826.
(35) Sünkel, K.; Schloter, K.; Beck, W.; Ackermann, K.; Schubert, U. *J. Organomet. Chem.* **1983**, *241*, 333.
(36) Wong, W. K.; Chiu, K. W.; Wilkinson, G.; Galas, A. M. R.; Thorton-Pett, M.; Hursthouse, M. B. *J. Chem. Soc., Dalton Trans.* **1983**, 1557.
(37) Ferguson, G. S.; Wolczanski, P. T. *J. Am. Chem. Soc.* **1986**, *108*, 8293.
(38) Morrison, E. D.; Bassner, S. L.; Geoffroy, G. L. *Organometallics* **1986**, *5*, 408.
(39) Fischer, E. O.; Kiener, V.; Burnbury, D. St. P.; Frank, E.; Lindley, P. F.; Mills, O. S. *Chem. Commun.* **1968**, 1378.
(40) Merlino, S.; Montagnoli, G.; Braca, G.; Sbrana, G. *Inorg. Chim. Acta* **1978**, *27*, 233.
(41) Kampe, C. E.; Boag, N. M.; Kaesz, H. D. *J. Am. Chem. Soc.* **1983**, *105*, 2896.
(42) Nishijima, M.; Yoshinobu, J.; Sekitani, T.; Onchi, M. *J. Chem. Phys.* **1989**, *90*, 5114.
(43) Blackman, G. S.; Kao, C. T.; Bent, B. E.; Mate, C. M.; van Hove, M. A.; Somorjai, G. A. *Surf. Sci.* **1988**, *207*, 66.
(44) Brown, N. F.; Barteau, M. A. *J. Am. Chem. Soc.* **1992**, *114*, 4258.
(45) Sekitani, T.; Takaoka, T.; Fujisawa, M.; Nishijima, M. *J. Phys. Chem.* **1992**, *96*, 8468.
(46) Stenhagen, E.; Abrahamsson, S.; McLafferty, F. W. *Atlas of Mass Spectral Data*; Wiley: New York, 1969.
(47) Sbrana, G.; Schettino, V. *J. Mol. Spectrosc.* **1970**, *33*, 100.
(48) Nuffel, P. V.; Enden, L. V. D.; Alsenoy, C. V.; Geise, H. J. *J. Mol. Struct.* **1984**, *116*, 99.
(49) Jo, M.; Kuwahara, Y.; Onchi, M.; Nishijima, M. *Solid State Commun.* **1985**, *55*, 639.
(50) Ellis, T. H.; Morin, M. *Surf. Sci.* **1989**, *216*, L351.
(51) Zaera, F.; Hall, R. B. *Surf. Sci.* **1987**, *180*, 1.
(52) Liu, Z.-M.; Zhou, X.-L.; Buchanan, D. A.; Kiss, J.; White, J. M. *J. Am. Chem. Soc.* **1992**, *114*, 2031.
(53) Delbecq, F.; Sautet, P. *Langmuir* **1993**, *9*, 197.
(54) Delbecq, F.; Sautet, P. *Surf. Sci.* **1993**, *295*, 353.
(55) Lloyd, K. G.; Roop, B.; Campion, A.; White, J. M. *Surf. Sci.* **1989**, *214*, 227.
(56) Godbey, D.; Zaera, F.; Yeates, R.; Somorjai, G. A. *Surf. Sci.* **1986**, *167*, 150.